biomass

MDPI

Article

Phycoremediation of Copper by *Chlorella prototheco*ides (UTEX 256): Proteomics of Protein Biosynthesis and Stress Response

Lidiane Maria Andrade [1,*], Caique Alves Tito [1], Camila Mascarenhas [1], Fabíola Aliaga Lima [1], Meriellen Dias [1], Cristiano José Andrade [2], Maria Anita Mendes [1] and Claudio Augusto Oller Nascimento [1]

[1] Dempster MS Lab, Chemical Engineering Department of Polytechnic School of University of São Paulo (USP), R. do Lago, 250–Butantã, São Paulo 05338-110, SP, Brazil; caique.tito@gmail.com (C.A.T.); cmascarenhasflorentino@gmail.com (C.M.); faaliaga@gmail.com (F.A.L.); meriellend@gmail.com (M.D.); mariaanita.mendes@gmail.com (M.A.M.); oller@usp.br (C.A.O.N.)

[2] LiEB, Integrated Laboratory of Biological Engineering, Department of Chemical Engineering and Food Engineering, Federal University of Santa Catarina (UFSC), R. do Biotério Central, S/n–Córrego Grande, Florianópolis 88040-970, SC, Brazil; eng.crisja@gmail.com

* Correspondence: lidiane.andrade@alumni.usp.br

Abstract: Phycoremediation is an eco-friendly treatment for mining wastes. Copper at high concentrations is toxic for microalgae growth (bioremediation). Proteomics is a modern approach that can assist in elucidating, in detail, the highly complex metabolic mechanisms related to phycoremediation. Therefore, this study aimed to evaluate the effect of copper ions (Cu^{2+}) on the metabolism of *Chlorella prototheco*ides (UTEX 256), particularly the proteome changes. The WC culture medium supplemented with Cu^{2+} at 0.3, 0.6, and 0.9 mg/L showed a strict correlation to Cu^{2+} removal of 40, 33, and 36% of the initial content, respectively. In addition, Cu^{2+} concentrations did not affect microalgae growth—a very traditional approach to measuring toxicity. However, the proteomics data indicated that when compared to the control, reductions in protein levels were observed, and the 10 most scored proteins were related to the light-harvesting complex. Interestingly, *C. prototheco*ides cultivated at 0.9 mg of Cu^{2+}/L biosynthesized the protein Ycf3-interacting chloroplastic isoform X1 to respond to the photooxidative stress and the DNA-directed RNA polymerase III subunit RPC5 was related to the Cu^{2+} binding. Pre-mRNA-processing factor 19 and cytochrome c peroxidase proteins were observed only in the copper-containing treatments indicating the activation of antioxidant mechanisms by reactive oxygen species, which are potential environmental pollutant biomarkers.

Keywords: mining waste; photooxidative stress; antioxidant metabolism; biomarkers

Citation: Andrade, L.M.; Tito, C.A.; Mascarenhas, C.; Lima, F.A.; Dias, M.; Andrade, C.J.; Mendes, M.A.; Nascimento, C.A.O. Phycoremediation of Copper by *Chlorella prototheco*ides (UTEX 256): Proteomics of Protein Biosynthesis and Stress Response. *Biomass* **2022**, *2*, 116–129. https://doi.org/10.3390/biomass2030008

Academic Editor: Giorgos Markou

Received: 1 April 2022
Accepted: 16 June 2022
Published: 23 June 2022

1. Introduction

Global mining waste is projected to grow from the 68.76 million tons generated in 2017 to approximately 87 million tons by 2022 [1]. Mining waste draws the attention of environmental agencies, particularly with regard to its proper treatment and disposal since it is composed of toxic elements [2,3].

Bioremediation, an interesting alternative to waste treatment, applies microorganisms or their metabolites to degrade, transform, remove, and/or reduce contaminants in an environmental matrix such as mining wastewater. Bioremediation is also a lower-cost remediation process than the current technologies used for toxic industrial waste removal [4,5]. In addition, bioremediation is environmentally friendly and provides high efficiency and adaptability [6]. Furthermore, current technologies are expensive and frequently ineffective at removing very low heavy metal concentrations [7,8].

Regarding microbial remediation, plenty of attention has been drawn to microalgae due to their fast growth in wastewater or wasteland, versatile metabolism, biodiversity, and consequent variability in their biochemical composition, combined with genetic improvements and the establishment of large-scale cultivation technologies [9,10]. Moreover,

phycoremediation can be integrated into the biosynthesis of value-added products (pigments, lipids, and amino acids, among others).

The phycoremediation of heavy metals has been carried out using microalgae, such as *Dunaliella tertiolecta*, *Chlorella pyrenoidosa*, or *Scenedesmus obliquus*, either in industrial or domestic wastewater treatment [11–16], since these microalgae can hyperaccumulate Cd, Cu, and Zn [17–20].

Microalgae can also be applied to remediate or recover heavy metals, which are cofactors for many enzymes, particularly enzymes related to the transport of photosynthetic electrons [21,22]. In addition, heavy metals naturally found in the environment have a wide range of oxidation states and coordination numbers that are associated with their toxicity.

In this sense, Ni and Cd at $\geq$2 mg/L affect microalgal growth [23–25]. The Cu is also toxic at high concentrations since it induces microalgal oxidative stress affecting algal photoprotection mechanisms and photosynthesis, pigment synthesis respiration processes, fatty acid production, and CO_2 fixation processes, and it also alters protein production [26–29].

The heavy metal toxicity in microorganisms is usually related to oxidative stress since heavy metals increase the concentrations of reactive oxygen species (ROS), thus leading to an unbalanced cellular redox status [30,31].

Proteomics consists of identifying and determining the functions of all proteins expressed in a cell, tissue, organism, or physiological fluid in a given biological situation [32]. It is a modern approach to the new and deep information on proteins expressed by microorganisms when subjected to a stress condition. It is worth noting that currently, proteomics is one of the best analytical strategies to investigate deeply the microalgae's heavy metal tolerance and its removal capacity and, in particular, to identify environmental biomarkers [32–35]. However, the metabolic mechanisms of phycoremediation related to the toxicity and removal of heavy metals are still virtually unknown [33–35].

Thus, the comparative proteomic analysis of samples from different environmental conditions allows a correlation between different protein expressions with toxic agents, for instance, heavy metals. In addition, these expressed proteins can be related to metabolic pathways [36]. Therefore, this work aims to investigate the metabolic effect of Cu^{2+} on *C. prototheco*ides (UTEX 256), in particular, microalgae growth; Cu^{2+} removal; and protein expressions related to (I) the protein biosynthesis process, (II) antioxidant activity, (III) copper-related proteins, and (IV) the response to stress, including potential environmental biomarkers.

2. Materials and Methods

*2.1. Chlorella Prototheco*ides *and Culture Conditions of the Stock Culture*

The *C. prototheco*ides (UTEX 256) microalgae were acquired from the UTEX Culture Collection of Algae, the University of Texas at Austin. The stock culture was continuously maintained (basal metabolism) in WC medium [37] at 23 °C, LED (Light Emitting Diode) intensity 4 µmol.photons/m^2.s from LED lamps (blue and red), and photoperiod 12/12 h L/D.

2.2. Quantitation by Chlorophyll

The microalgae were previously acclimatized (pre-inoculum) by using 100 mL WC medium [37], 30 °C [38], rotation of 150 rpm (109/1TC, Ethik Technology, Vargem Grande Paulista, São Paulo, Brazil), initial optical density at 665 nm (OD_{665nm}) = 0.1 (acclimatized), and LED intensity 20 µmol.photons.m^{-2}.s^{-1} red and blue).

After the pre-inoculum the microalgae in the exponential growth phase were used as inoculum, taking as standard the 4th day (after 72 h, OD_{665nm} is higher than 0.4) to decrease the adaptation phase during the crops [39].

Then, the microalgae growth using the same pre-inoculum conditions, was conducted in duplicate. Sampling every two days was carried out, in which 2 mL of microalgae suspension was collected and used to read OD at 665 nm and for chlorophyll extraction.

The cell suspensions were centrifuged at 4000 rpm for 3 min (5840 R centrifuge, Eppendorf, Hamburg, Hamburg, Germany) and the supernatant was completely removed. Then, 2 mL of methanol was added, agitated using a vortex for 1 min, and centrifuged at 4000 rpm for 3 min (5840 R centrifuge, Eppendorf, Hamburg, Germany). The extracted chlorophyll's supernatant was carried out by absorbance measurements (OD_{665nm}) (UV2600, Shimadzu, Quioto, Quioto, Japan).

The correlations between OD_{665nm} and chlorophyll quantity (ug) are given by using Mackinney's empirical equation (Equation (1)) [40].

$$\mu g_{chlorophyll}/mL_{medium} = (13.43.A_{665}.\nu)/(l.V) \quad (1)$$

where:

A_{665}–absorbance at 665 nm
ν–volume of methanol (mL)
l–spectrophotometric cell length (cm)
V–volume of sample (mL)

Chlorophyll content has a direct linear correlation to cell growth. For the chlorophyll extraction quantification, the experiments were performed in duplicate, and the average absorbances at 665 nm were applied in Mackinney's empirical equation. Thus, the content of extracted chlorophyll can be precisely related to the absorbance at 665 nm through Equation (2).

$$\mu g_{chlorophyll} = 0.0548.A_{665nm} \quad (2)$$

2.3. Growth Curves

Previously acclimatized (as described above), the *C. protothecoides* microalgae were growth in 100 mL WC medium [37] supplemented with copper at different concentrations (0 (Control), 0.3, 0.6, and 0.9 mg of Cu^{2+}/L) at 30 °C [38], 150 rpm, initial OD_{665nm} = 0.1 (acclimatized), and LED intensity 20 μmol.photons/m^2.s.

The 10 day cultivations were performed in duplicate. Samples were collected every 2 days and analyzed in a spectrophotometer (UV 2600–Shimadzu) at 665 nm (chlorophyll reading). Then, microalgae suspensions were centrifuged at 4000 rpm for 3 min (5840 R centrifuge, Eppendorf, Hamburg, Hamburg, Germany), and the supernatant was stored at 4 °C for further copper adsorption analysis.

After 10 days, the microalgae biomasses were washed with Milli-Q water 3 times, centrifuged at 4000 rpm for 3 min (5840 R centrifuge, Eppendorf, Hamburg, Hamburg, Germany), and lyophilized until further digestion and analysis (proteome).

2.4. Copper Removal Capacity by C. protothecoides

The evaluation of Cu^{2+} removal was carried out by analyzing supernatants (*C. protothecoides* UTEX 256 cultivation).

The samples were stored at −18 °C. Quantification was performed using a Flame Atomic Absorption Spectrometer (FAAS) (GFA–7000a, Shimadzu, Kyoto, Kyoto, Japan) containing a hollow-cathode lamp with a specific copper wavelength at 324.75 nm (Hamamatsu Photonics K.K., Hamamatsu, Shizuoka, Japan) and a flame detector using acetylene gas and compressed air.

The supernatants were submitted to defrosting at room temperature for the remaining Cu^{2+} determinations. The operating parameters of analytical instrumentation were performed according to the manufacturer's recommendations and also adapted from Abreu et al. [34]. To determine metal ions in the supernatant, the samples were acidified with HNO_3 (final concentration at 2% v/v) ranging from 0.05 to 1 mg/L, suitable for the detector set-up.

The Cu^{2+} adsorption efficiency (%) was calculated according to Equation (3) [41].

$$Abs_R\ (\%) = ((C_0 - C_S)/C_0) \times 100 \quad (3)$$

where

C_s: Concentration of Cu^{2+} in the solution (mg Cu^{2+}/L)
C_0: Initial concentration of Cu^{2+} in the solution (mg Cu^{2+}/L)

2.5. Tryptic Digestion for Mass Spectrometry Analysis

Trypsin solution was prepared using the bovine pancreas trypsin enzyme (Sigma Aldrich, St. Louis, MI, USA), which was solubilized in 400 µL of 50 mM ammonium bicarbonate solution (NH_4HCO_3) to reach a final concentration of 0.05 ng of enzyme/nL of solution [29]. The tryptic digestion was performed using 0.2 mg of lyophilized samples (freeze-dryer model Freezone 4.5, LabConco, Kansas City, MI, USA), adding 50 µL trypsin solution (0.05 ng/nL), and then incubating at 37 °C for 18 h [29]. After this period, the digestion process was interrupted by the addition of 10 µL of 10% (*v*/*v*) trifluoroacetic acid, and the solution was kept at 37 °C for another 90 min, followed by centrifugation for 30 min at 6 °C, 17,400 g (CT15RE, Himac, Hitachinaka, Ibaraki, Japan), and then the supernatant containing the digested proteins was transferred to vials containing inserts for subsequent analysis.

2.6. Protein Identification by NanoLC-ESI-Q-TOF System

Protein identification was performed using the high-efficiency liquid nanochromatography technique coupled to mass spectrometry using a nanoLC-ESI-Q-TOF system (NanoLC model UltiMate 3000 from Thermo Fisher Scientific, Waltham, MA, USA, and ESI-Q-TOF model Impact II from Bruker Corporation, Billerica, MA, USA) containing a nanoelectrospray ionization source and TOF quadrupole mass analyzer. An amount of 1 µL of digested peptides was separated in a PepMap nanocolumn (C18, 5 µm particles, 300 Å pore size, 15 cm long, 75 µm internal diameter; Thermo Scientific) under a gradient from 2 to 98% (*v*/*v*) acetonitrile (Sigma-Aldrich) containing 0.1% formic acid for 180 min at a flow rate of 0.3 µL/min.

The mass spectrometry (ESI-Q-TOF), previously calibrated with a tuning mix solution (Agilent, Santa Clara, CA, USA), was operated with ionization in positive-ion mode, and the spectra of precursor ions (MS) were acquired in the range of 50–3000 m/z with an acquisition frequency of 2 Hz, capillary voltage of 1.5 kV, source temperature of 150 °C, drying gas flow of 3 L/min, and nebulizer pressure of 0.2 bar. The precursor ion fragments (MS/MS) were acquired with an acquisition frequency of 4 to 16 Hz and collision energy between 7 and 70 eV. The mass spectra obtained were integrated and processed using DataAnalysis 4.3.

2.7. Peaks Database Searching

Data file analysis (d) from Bruker mass spectrometers was performed in PEAKS Studio 10.5 software (Bioinformatics Solutions Inc., Waterloo, ON, Canada). MS/MS spectra were submitted for de novo analysis and database search using peaks DB, PTM, and Spider tools [42]. For the analysis, 20 ppm precursor mass tolerance, 0.025 Da fragment mass tolerance, and false discovery rates (FRD) for protein and peptides at a maximum of 1% were used. All the identified proteins had at least one unique peptide and were analyzed through the UniProt classification system. Gene ontology (GO) relationships were used to group proteins by molecular function and biological process in a wide-ranging way to accurately predict protein function.

C. protothecoides has a low number of proteins (20,946). The *Chlorella* genus was used, which has 69,943 proteins in the Uniprot database (downloaded on 29 July 2020).

2.8. Statistical Analysis

Excel 2019 software (Microsoft, Redmond, Washington, DC, USA) was used for statistical analyses, calculation of means, standard deviation (SD), coefficient of variation (cv%), and correlation coefficients. The UV readings for chlorophyll quantitation and microalgae growth curves were performed twice while FAAS analysis was conducted. The tryptic

digestion and mass spectrometry analysis were performed twice and the mass spectra obtained were integrated and processed using DataAnalysis 4.3 version (Bruker Daltonics, Billerica, MA, USA). For database search of the protein analysis (peaks DB, PTM, and Spider tools), the PEAKS Studio 10.5 software was used (Bioinformatics Solutions Inc., Walterloo, ON, Canada).

All identified proteins (MS data) were analyzed on the UniProt classification system using the UniProtKB Pathway tool related to the protein biosynthesis process, and the UniProtKB gene ontology (GO) analysis tool to group proteins by molecular function antioxidant activity, which includes the antioxidant and peroxidase categories, and also by binding-ion binding-cation binding-transition metal-copper to analyze copper-related proteins. To evaluate response to stress proteins, a category in the GO biological process-response to stimulus, was analyzed.

3. Results

3.1. Growth Curves

The *C. protothecoides* growth curves at different Cu^{2+} concentrations are shown in Figure 1.

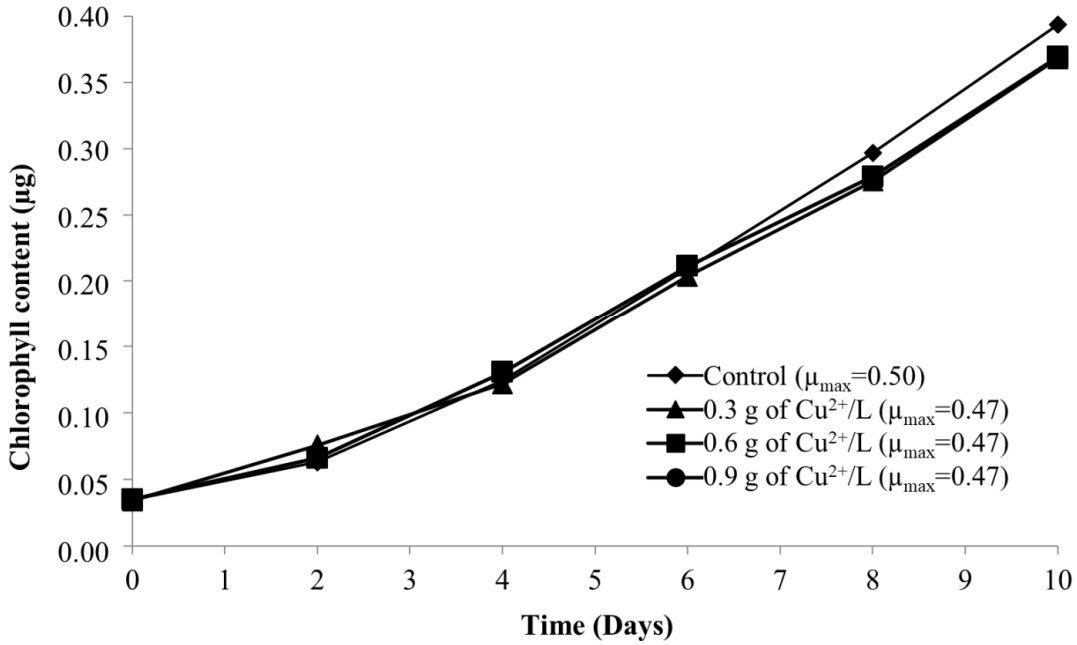

Figure 1. *C. protothecoides* growth curves.

After 10 days, all cultivations were the in exponential phase, that is, the period of the highest protein production. According to Pradeep et al. [43], the microalgae growth rate is not affected by copper (up to 4 mg of Cu^{2+}/L). However, a subtle difference (0.03 day^{-1}) was observed in the μ_{max} value due to copper since the μ_{max} values for control and copper treatment cultures were 0.47 and 0.50 day^{-1}, respectively.

3.2. Copper Removal Capacity by C. protothecoides

The copper removal capacity curves using the supernatants of the cultures after 10 days were analyzed by FAAS and the results are shown in Figure 2. The samples containing copper (II) (0.3, 0.6, and 0.9 mg/L) showed a similar copper removal of ≈30–40%, that is, 0.12, 0.20, and 0.32 mg/L, respectively.

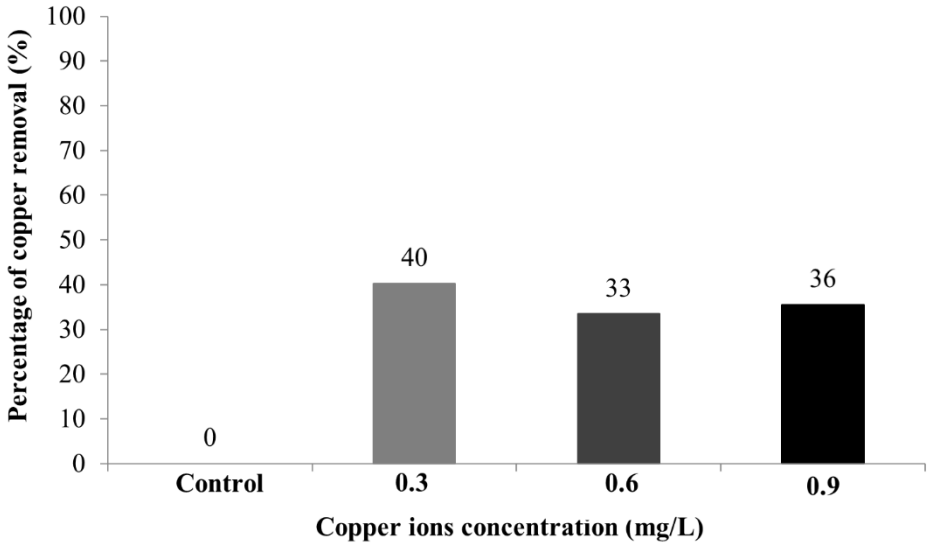

Figure 2. Copper removal capacity by *C. protothecoides*.

3.3. Protein Identification by NanoLC-ESI-Q-TOF System

Among the 10 most scored proteins (Table 1), mainly proteins related to the light-harvesting complex (LHC), such as chlorophyll a-b binding, photosystem II CP43, photosystem II CP47, photosystem II protein D1, photosystem II protein D2, ATP synthase subunit beta, ATP synthase subunit alpha, and ribulose-bisphosphate carboxylase large chain, were observed.

Based on proteomics data from microalgal cultivation data, the Venn diagram was developed (Figure 3). The proteomic data analysis indicated 309 common proteins for all cultivations including the control.

Table 1. Identified proteins according to the ten highest scores for control and Cu^{2+} treatments.

Sample	Uniprot Access	Score	Molecular Mass (Da)	No. of Peptides	Protein
Control	A0A2P6TDA6_CHLSO	302.46	26,968	27	Chlorophyll a-b binding protein
	ATPB_CHLVU	295.87	51,644	31	ATP synthase subunit beta
	PSBC_CHLVU	287.16	52,048	30	Photosystem II CP43 reaction center protein
	Q85YT9_CHLVU	277.71	49,722	26	Ribulose-bisphosphate carboxylase large chain
	A9XHZ1_CHLVU	271.19	70,833	25	Heat shock 70
	PSBB_CHLVU	271.16	56,130	24	Photosystem II CP47 reaction center protein
	ATPA_CHLVU	253.95	54,709	25	ATP synthase subunit alpha
	PSBA_CHLVU	247.13	38,986	16	Photosystem II protein D1
	CYF_CHLVU	235.09	34,213	16	Cytochrome f
	PSBD_CHLVU	230.53	39,429	15	Photosystem II D2 protein
0.3mg of Cu^{2+}/L	A0A2P6TDA6_CHLSO	297.06	26,968	24	Chlorophyll a-b binding protein
	PSBC_CHLVU	281.31	52,048	26	Photosystem II CP43 reaction center protein
	A9ZM90_CHLVU	281.15	52,490	29	Ribulose-bisphosphate carboxylase large chain
	A9XHZ1_CHLVU	266.36	70,833	26	Heat shock 70
	ATPB_CHLVU	265.86	51,644	28	ATP synthase subunit beta
	PSBB_CHLVU	259.39	56,130	25	Photosystem II CP47 reaction center protein
	ATPA_CHLVU	253.66	54,709	28	ATP synthase subunit alpha
	PSBA_CHLVU	237.31	38,986	18	Photosystem II protein D1
	PSBD_CHLVU	234.49	39,429	15	Photosystem II D2 protein
	PSAA_CHLVU	224.73	83,227	21	Photosystem I P700 chlorophyll an apoprotein A1

Table 1. *Cont.*

Sample	Uniprot Access	Score	Molecular Mass (Da)	No. of Peptides	Protein
0.6 mg of Cu^{2+}/L	A0A2P6TDA6_CHLSO	317.52	26,968	20	Chlorophyll a-b binding protein
	F2YGQ1_CHLVA	288.18	52,167	26	Photosystem II CP43 reaction center protein
	A9ZM90_CHLVU	284.66	52,490	28	Ribulose bisphosphate carboxylase large chain
	ATPB_CHLVU	278.65	51,644	29	ATP synthase subunit beta
	A9XHZ1_CHLVU	272.86	70,833	25	Heat shock 70
	PSBB_CHLVU	267.41	56,130	26	Photosystem II CP47 reaction center protein
	ATPA_CHLVU	264.82	54,709	23	ATP synthase subunit alpha
	PSBA_CHLVU	252.26	38,986	18	Photosystem II protein D1
	A0A345 × 1B8_CHLVU	250.01	20,493	17	Photosynthesis I subunit
	PSBD_CHLVU	241.49	39,429	14	Photosystem II D2 protein
0.9 mg of Cu^{2+}/L	A0A2P6TDA6_CHLSO	312.92	26,968	21	Chlorophyll a-b binding protein
	A9ZM90_CHLVU	266.08	52,490	22	Ribulose bisphosphate carboxylase large chain
	PSBC_CHLVU	264.92	52,048	22	Photosystem II CP43 reaction center protein
	PSBB_CHLVU	263.61	56,130	23	Photosystem II CP47 reaction center protein
	A9XHZ1_CHLVU	255.53	70,833	19	Heat shock 70
	PSBA_CHLVU	244.60	38,986	15	Photosystem II protein D1
	ATPA_CHLVU	243.16	54,709	21	ATP synthase subunit alpha
	ATPB_CHLVU	242.18	51,644	24	ATP synthase subunit beta
	Q9SLP7_CHLVU	239.30	10,804	13	Antifreeze protein
	A0A3M7KX29_AUXPR	232.79	217,317	11	Histone acetyltransferase
	A0A2P6TDA6_CHLSO	312.92	26,968	21	Chlorophyll a-b binding protein

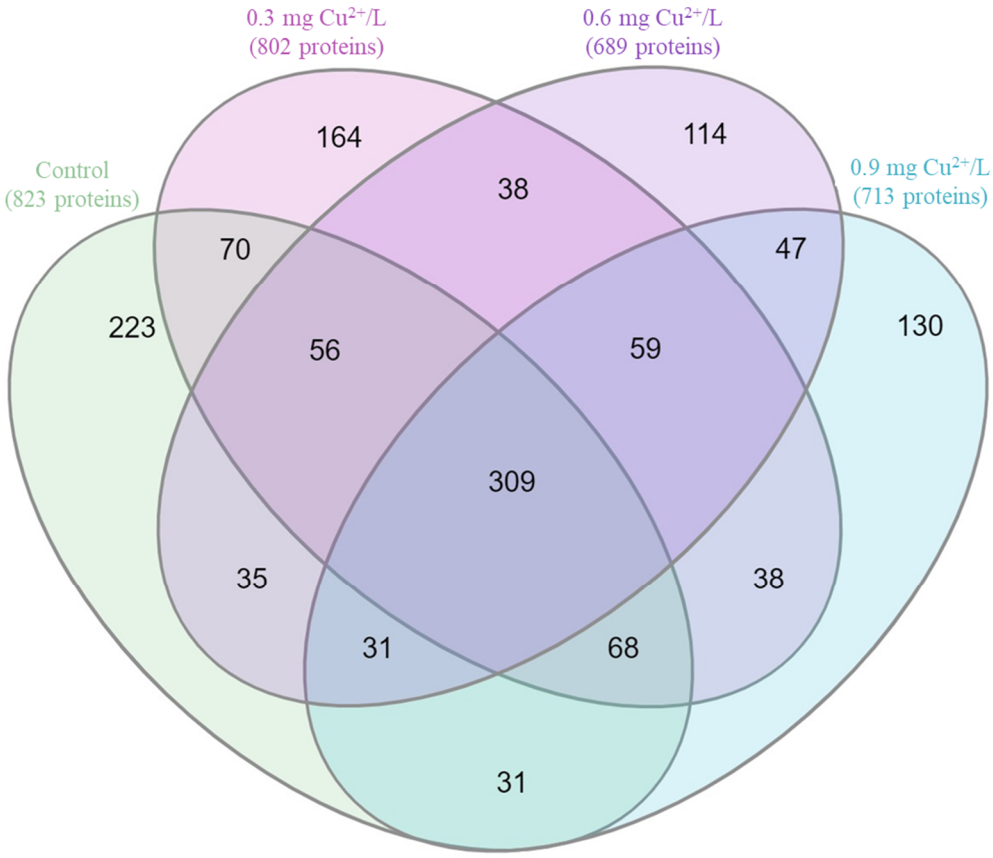

Figure 3. Venn diagram of identified proteins from control and copper treatments (0.3, 0.6, and 0.9 mg of Cu^{+2}/L) using the Venny tool [44].

The analysis using the UNIPROT Database of identified proteins by the UniProtKB Pathway tool related to the protein biosynthesis process confirmed the reduction of protein biosynthesis when increasing the Cu^{2+} concentration (Table 2).

Table 2. Identified proteins related to protein biosynthesis.

Protein	Control	0.3 mg of Cu^{2+}/L	0.6 mg of Cu^{2+}/L	0.9 mg of Cu^{2+}/L
ENTH domain-containing protein	+	+	-	-
Dihydroxy-acid dehydratase	+	+	-	-
Elongation factor G	+	+	+	+

- Protein absent; + 1 Identified protein.

Proteomic data analysis by selecting the GO molecular function antioxidant activity, which includes the peroxidase activity category (Px), indicated the presence of ≈7 proteins, whereas superoxide dismutase (SOD) indicates 2 proteins, as shown in Table 3.

Table 3. Identified proteins related to antioxidant activity including Px and SOD.

	Protein	Control	0.3 mg of Cu^{2+}/L	0.6 mg of Cu^{2+}/L	0.9 mg of Cu^{2+}/L
Px	Ascorbate peroxidase	+	+	+	+
	Catalase	+	-	+	-
	Cytochrome c peroxidase	-	+	+	+
	Glutaredoxin-dependent peroxiredoxin	+	+	+	+
	L-ascorbate peroxidase	+	+	+	++
	Peroxidase 4 domain-containing protein	+	+	+	+
	Putative L-ascorbate peroxidase chloroplastic isoform X1	+	+	+	+
SOD	Superoxide dismutase	++	++	++	+
	30S ribosomal protein S17	-	-	-	+

GO molecular functions binding ion, binding cation, binding transition, metal copper showed the presence of the highest copper content cultivation of DNA-directed RNA polymerase III subunit RPC5 protein, which is related to the Cu^{2+} binding. - Protein absent; + 1 Identified protein; ++ 2 Identified proteins.

Regarding the response to stress, a category in the GO biological process response to stimulus, cultivation in the absence of copper, showed 17 proteins, of which five are related to oxidative stress. On the other hand, the microalgal cultivation doped with Cu^{2+} expressed between 19 and 23 responses to stress proteins and showed a slight increase in proteins correlated to the stress response (Table 4).

Table 4. Identified proteins related to response to stress.

Protein	Control	0.3 mg of Cu^{2+}/L	0.6 mg of Cu^{2+}/L	0.9 mg of Cu^{2+}/L
30S ribosomal protein S17 *	-	-	-	+
Acetolactate synthase	+	-	+	-
Ascorbate peroxidase *	+	+	+	+
Catalase *	+	-	+	-

Table 4. *Cont.*

Protein	Control	0.3 mg of Cu^{2+}/L	0.6 mg of Cu^{2+}/L	0.9 mg of Cu^{2+}/L
Chaperone chloroplastic-like	-	+	+	+
Clp R domain-containing protein	-	-	+	-
Cytochrome c peroxidase *	-	+	+	+
Deoxyribodipyrimidine photo-lyase	+	-	-	-
DNA_MISMATCH_REPAIR_2 domain-containing protein	+	+	+	+
DnaJ-like protein	-	-	+	-
Flagellar outer dynein arm heavy chain beta	+	+	+	+
General transcription and DNA repair factor IIH helicase subunit XPD	+	+	+	+
Hsp100 family	+	+	+	+
L-ascorbate peroxidase *	+	+	+	++
Peptide-methionine (R)-S-oxide reductase *	+	-	+	+
Peroxidase-4-domain-containing protein *	+	+	+	+
Photosystem II protein D1	+	+	+	+
Pre-mRNA-processing factor 19	-	+++	+++	+++
Superoxide dismutase *	++	++	++	+
Thioredoxin reductase *	+	+	-	-
Ubiquitin receptor RAD23	-	++++	-	++
Uncharacterized E1ZQY5	+	-	+	-
Uncharacterized E1Z452	-	-	+	-
Uncharacterized E1Z369 *#	-	-	-	+
Uracil-DNA glycosylase	+	+	+	+
Ycf3-interacting chloroplastic isoform X1 *#	-	-	-	+

* Protein correlated to oxidative stress; # Protein correlated to photo-oxidative stress. - Protein absent; + 1 Identified protein; ++ 2 Identified proteins; +++ 3 Identified proteins; ++++ 4 Identified proteins.

4. Discussion

4.1. Growth Curves

During the 10 day cultivation, all experiments were in the exponential phase, similar to that described by Andrade et al. [45]. This difference can be explained due to the use of LED light, which increases microalgae growth. A subtle difference (0.03 day^{-1}) was observed in the μ_{max} value due to Cu^{2+}, since the μ_{max} values for control and copper treatment cultures were 0.47 and 0.50 day^{-1}, respectively.

Under the present experimental conditions, a Cu^{2+} concentration of up to 0.9 mg of Cu^{2+}/L does not limit the specific growth rate and does not inhibit *C. protothecoides* microalgae growth.

4.2. Copper Removal Capacity by C. protothecoides

The experiments were conducted for 10 days to certify the Cu^{2+} removal by *C. protothecoides* microalgae. The samples containing Cu^{2+} (0.3, 0.6, and 0.9 mg/L) showed copper removal of 0.12, 0.20, and 0.32 mg/L, respectively, which accounts for 40, 30, and 36% of the initial Cu^{2+} content. *C. protothecoides* showed remarkable adaptability to Cu^{2+} since the highest copper concentration led to a higher copper removal level. Thus, the concentrations evaluated are not toxic for microalgae growth, which can corroborate that there have been no changes in its cell growth.

Sabatini et al. [46] reported that the first response by microalgae for decreasing the toxic effect of copper is to strongly bind copper ions to the cellular walls. Thus, no effect on

microalgal growth was observed. However, in the present study, similar growth curves in all experiments were observed since a subtle difference among the μ_{max} values for the control and copper treatment cultures, 0.47 and 0.50 day^{-1}, respectively, was due to the presence of Cu^{2+} (Figure 1).

The accumulation of copper (0.001 to 0.05 mg/L) by three freshwater microalgae was studied by Guanzon et al. [47]. They observed removal rates between 30 and 45% day^{-1} and that the blue-green algae showed the highest amount of absorbed copper of about 480 μg of Cu/g dry weight with an initial solution containing 50 μg of Cu^{2+}/L. In a more recent study, Abreu et al. [34] evaluated the effects of cadmium and copper in the *Chlorella vulgaris* growth and its potential heavy metal removal. They found that approximately 35% (75 μg) of the copper initially present in the culture medium (211 μg) was accumulated in the microalgae biomass. Both results corroborate the present study (30 and 40% removal of initial Cu^{2+} content).

4.3. Protein Identification by NanoLC-ESI-Q-TOF System

The 10 most scored proteins, as shown in Table 1, are mainly related to the light-harvesting complex (LHC) such as chlorophyll a-b binding, photosystem II CP43, photosystem II CP47, photosystem II protein D1, photosystem II protein D2, ATP synthase subunit beta, ATP synthase subunit alpha, and ribulose-bisphosphate carboxylase large chain.

Chlorophyll a-b binding protein is responsible for light reception and also for the capture and delivery of excitation energy to photosystem II (PSII). Located in the thylakoid membrane, PSII, also known as water: plastoquinone oxidoreductase, is a membrane protein complex that starts with the light-dependent reactions of oxygenic photosynthesis, capturing the photons from the source energy to catalyze water molecules to obtain molecular oxygen and protons (H^+). The protons will be converted into a biologically useful chemical (ATP) [48–50].

Photosystem II CP43 reaction center protein is a component of the core complex photosystem II (PSII) which binds the chlorophyll and assists with catalyzing the primary light-induced photochemical process of PSII. Photosystem II protein D1 binds the main electron donor of PSII P680 (reaction center pigment), and photosystem II protein D2 is necessary for the stability of PSII [50].

ATP synthase subunit alpha and ATP synthase subunit beta proteins produce ATP from ADP when in the presence of a proton gradient across the membrane. The alpha chain is a regulatory subunit, whereas the beta chain primarily hosts the catalytic sites [50].

Ribulose-bisphosphate carboxylase large chain has a molecular function of magnesium ion binding, which is also involved in PSII forming the central atom of chlorophyll [50].

Cytochrome f protein, which mediates the transfer of electrons between PSII and PSI (photosystem I), cyclic electric flow around PSI, and state transition, only appears (among the top ten) in the control sample [50].

Heat shock 70 (HSP70) plays a role in ATP binding and was also described as an immunoreactive protein acting as a cytokine and activating immune cells [50,51].

Treatments containing 0.3 and 0.6 mg of Cu^{2+}/L presented proteins related to the PSI, such as photosystem I P700 chlorophyll, an apoprotein A1 and photosynthesis I subunit, which, respectively, bind the P700 (reaction center pigment of PSI) and encode an abundant protein of the PSI.

The highest copper content sample showed the presence of histone transferase protein, which is involved in several metabolic processes such as transcription activation and DNA repair [52]. Those results can be confirmed by the 10 identified proteins that present higher scores, as shown in Table 1.

From the microalgal cultivation data, the Venn diagram was developed (Figure 3). The proteomic data analysis indicated 309 common proteins for all cultivations including the control. These proteins are very likely strictly related to essential pathways such as central (energetic) pathways (glycolysis and Krebs cycle).

It is well-known that copper plays a significant role in microalgae metabolism, in particular, in the stability of proteins, synthesis of pigments, lipid membranes, processes of photosynthesis, and respiration. Copper inhibited the biosynthesis of proteins (types). Compared to the control, the cultivation at 0.3, 0.6, and 0.9 mg of Cu^{2+}/L led to a reduction in proteins (types) of 2.6, 16.3, and 13.4%, respectively. Moreover, all identified proteins, analyzed through the UniProt classification system using the UniProtKB Pathway tool related to the protein biosynthesis process, showed a reduction in protein biosynthesis, mainly the ENTH domain-containing protein and the dihydroxy-acid dehydratase proteins (both involved in the pathway polypeptide chain elongation responsible for maintaining protein homeostasis) [53] with increasing copper concentrations (Table 2). Therefore, despite having a similar growth rate, Cu^{2+} negatively affects protein biosynthesis.

Other enzymes, such as Px and SOD, have been reported to be overexpressed in microalgae that were exposed to heavy metals. However, these enzymes could be related to the degradation of the contaminants or indirectly as a defensive stress response to assist the balance of cellular homeostasis through, for instance, the detoxification of ROS [54], which increase when the heavy metal content is toxic. The analysis of proteomic data by selecting the GO molecular function antioxidant activity, indicated ≈7 proteins related to Px and 2 SOD, as shown in Table 3. It should be noted that copper likely induced the biosynthesis of cytochrome c peroxidase (peroxidase activity). In other words, the antioxidant mechanisms (antioxidant enzymes) of *C. protothecoides* were activated by the production of ROS. It is worth noting that regarding the SOD enzymes, the downregulated 30S ribosomal protein S17 was identified in the highest copper content cultivation. In the biological system, downregulation is when a cell decreases the quantity of a cellular component, such as protein, in response to an external stimulus, such as the presence of heavy metals, for instance, copper. Enzymes related to peroxidase activity have been reported as highly sensitive to copper, including very low concentrations of 1.27 mg/L, as reported by Sauser et al. [55], corroborating with the present study with even lower copper concentrations.

In terms of the response to stress in the presence of copper even at low concentrations, a category in the GO biological process response to stimulus, cultivation in the absence of copper, showed 17 proteins, of which five are related to oxidative stress. Otherwise, the cultivation with copper content expressed between 19 and 23 responses to stress proteins and showed a slightly increased oxidative stress response associated with protein (Table 4).

Related to both SOD and stress responses, the downregulated 30S ribosomal protein S17 contributed to the structural integrity of the ribosome, the site of protein biosynthesis [49]. Additionally, the sample with the highest copper content (0.9 mg of Cu^{2+}/L) showed the presence of Ycf3-interacting chloroplastic isoform X1, a chloroplast-enhancing stress-tolerance protein, which was a response to the photooxidative stress. Additionally, the protein DNA-directed RNA polymerase III subunit RPC5, which is related to copper ion binding, was also observed only at the highest copper content.

Pre-mRNA-processing factor 19 protein, which appears only in the copper-containing treatments, is responsible for restoring DNA after damage due to chemical or physical agents. As previously described, cytochrome c peroxidase protein, related to both peroxidase and stress responses, was also observed for all the copper-containing cultivations. Both proteins (pre-mRNA-processing factor 19 and cytochrome c) showed potential environmental copper pollutant biomarkers for *C. protothecoides* even at low metal concentrations such as 0.3 mg of Cu^{2+}/L.

Thus, a deeper understanding of the cellular mechanisms related to heavy metal tolerance and removal is an interesting alternative for the enhanced management of copper-contaminated environments.

5. Conclusions

In conclusion, a copper concentration of up to 0.9 mg of Cu^{2+}/L does not affect the specific growth rate of *C. protothecoides* microalgae. However, the analysis of the

Venn diagram clearly showed that even at a low concentration, the copper inhibited the biosynthesis of proteins (types). The proteomic analysis indicated that the 10 most scored proteins found in all the cultivations are mainly related to the light-harvesting complex (LHC). Regarding peroxidases, a protein overexpressed by stressed microalgae, ≈7 proteins were identified (in all cultivations), in which the biosynthesis of cytochrome c peroxidase was observed in all the copper treatments. Thus, it indicates the activation of antioxidant mechanisms. Additionally, in the highest copper concentration treatment, the Ycf3-interacting chloroplastic isoform X1 protein was biosynthesized as a response to photooxidative stress and also the DNA-directed RNA polymerase III subunit RPC5 protein, which is related to copper ion binding. In conclusion, a simple growth rate analysis can lead to misinterpretation. The cytochrome c peroxidase and pre-mRNA-processing factor 19 are potential environmental copper pollutant biomarkers for *C. protothecoides*, even at low metal concentrations of 0.3 mg of Cu^{2+}/L.

Author Contributions: L.M.A. participated in the Conceptualization, Methodology, Formal Analysis, Investigation, Data curation, Visualization, Writing—Original draft preparation, and Project Administration. C.A.T., C.M., F.A.L. and M.D. assisted in the Methodology and Investigation. C.J.A. performed the Writing—Original draft preparation. M.A.M. and C.A.O.N. were responsible for Resources, Project Administration, and Funding acquisition. All authors read, reviewed, and approved the final manuscript. All authors have read and agreed to the published version of the manuscript.

Funding: This research was funded by Fundação de Amparo à Pesquisa do Estado de São Paulo (FAPESP) through the Research Project 2013/50218-2, Conselho Nacional de Desenvolvimento Científico e Tecnológico (CNPq) and Coordenação de Aperfeiçoamento de Pessoal de Nível Superior (CAPES).

Institutional Review Board Statement: Not applicable.

Informed Consent Statement: Not applicable.

Data Availability Statement: The data presented in this study are available on request from the corresponding author.

Conflicts of Interest: The authors declare no conflict of interest.

References

1. Technavio. *Global Mining Waste Management Market 2018–2022*; Technavio (Infinitti Research Ltd.): London, UK, 2018.
2. MacFarlane, G.; Burchett, M. Photosynthetic pigments and peroxidase activity as indicators of heavy metal stress in the Grey Mangrove, *Avicennia marina* (Forsk.) Vierh. *Mar. Pollut. Bull.* **2001**, *42*, 233–240. [CrossRef]
3. Kim, H.; Choi, W.J.; Maeng, S.K.; Kim, H.J.; Kim, H.S.; Song, K.G. Ozonation of piggery wastewater for enhanced removal of contaminants by *S. quadricauda* and the impact on organic characteristics. *Bioresour. Technol.* **2014**, *159*, 128–135. [CrossRef] [PubMed]
4. Rayu, S.; Karpouzas, D.G.; Singh, B.K. Emerging technologies in bioremediation: Constraints and opportunities. *Biodegradation* **2012**, *23*, 917–926. [CrossRef] [PubMed]
5. Hlihor, R.M.; Gavrilescu, M.; Tavares, T.; Favier, L.; Olivieri, G. Bioremediation: An overview on current practices, advances, and new perspectives in environmental pollution treatment. *BioMed Res. Int.* **2017**, *2017*, 6327610. [CrossRef]
6. Bulgariu, L.; Gavrilescu, M. Bioremediation of heavy metals by microalgae. In *Handbook of Marine Microalgae: Biotechnology Advances*; Kim, S.-K., Ed.; Academic Press: Amsterdam, The Netherlands, 2015; pp. 457–469.
7. Birungi, Z.S.; Chirwa, E.M.N. The adsorption potential and recovery of thallium using green micro-algae from eutrophic water sources. *J. Hazard. Mater.* **2015**, *299*, 67–77. [CrossRef] [PubMed]
8. Yaghmaeian, K.; Jaafari, J. Optimization of heavy metal biosorption onto freshwater algae (*Chlorella coloniales*) algae cells using response surface methodology (RSM). *Chemosphere* **2018**, *217*, 447–455. [CrossRef]
9. Kalra, R.; Gaur, S.; Goel, M. Microalgae bioremediation: A perspective towards wastewater treatment along with industrial carotenoids production. *J. Water Process Eng.* **2021**, *40*, 101794. [CrossRef]
10. Derner, R.B.; Ohse, S.; Villela, M.; Carvalho, S.M.; Fett, R. Microalgas, produtos e aplicações. *Cienc. Rural* **2006**, *36*, 1959–1967. [CrossRef]
11. Han, S.Q.; Zhang, Z.H.; Yan, S.H. Present situation and developmental trend of wastewater treatment and eutrophication waters purification with alga technology. *Agro-Environ. Develop.* **2000**, *63*, 13–16.
12. Olguin, E.J. Phycoremediation: Key issues for cost-effective nutrient removal process. *Biotechnol. Adv.* **2003**, *22*, 81–91. [CrossRef]
13. Kshirsagar, A.D. Bioremediation of wastewater by using microalgae: An experimental study. *Int. J. Life Sci. Biotechnol. Pharma Res.* **2013**, *2*, 339–346.

14. Andrade, C.J.; Andrade, L.M. An overview on the application of genus *Chlorella* in biotechnological processes. *J. Adv. Res. Biotechnol.* **2017**, *2*, 1–9. [CrossRef]
15. Andrade, C.J.; Andrade, L.M. Microalgae for bioremediation of textile wastewater: An overview. *MOJ Food Process. Technol.* **2018**, *6*, 432–433. [CrossRef]
16. Corrêa, P.S.; Teixeira, C.M.L.L.; Dantas, F.M.L. Reaproveitamento de resíduos da indústria de biodiesel para produção de biomassa microalgal. In Proceedings of the VI Workshop Redealgas, Arraial do Cabo, Brazil, 26–30 November 2017.
17. Ettajani, H.; Berthet, B.; Amiard, J.C.; Chevolot, L. Determination of cadmium partitioning in microalgae and oysters: Contribution to the assessment of trophic transfer. *Arch. Environ. Contam. Toxicol.* **2001**, *40*, 209–221. [CrossRef]
18. Tsuji, N.; Hirayanagi, N.; Iwabe, O.; Namba, T.; Tagawa, M.; Miyamoto, S.; Miyasaka, H.; Takagi, M.; Hirata, K.; Miyamoto, K. Regulation of phytochelatin synthesis by zinc and cadmium in marine green alga, *Dunaliella tertiolecta*. *Phytochemistry* **2003**, *62*, 453–459. [CrossRef]
19. Zhou, G.J.; Peng, F.Q.; Zhang, L.J.; Ying, G.G. Biosorption of zinc and copper from aqueous solutions by two freshwater green microalgae *Chlorella pyrenoidosa* and *Scenedesmus obliquus*. *Environ. Sci. Pollut. Res.* **2012**, *19*, 2918–2929. [CrossRef]
20. Kwon, H.K.; Jeon, J.Y.; Oh, S.J. Potential for heavy metal (copper and zinc) removal from contaminated marine sediments using microalgae and light emitting diodes. *Ocean Sci. J.* **2017**, *52*, 57–66. [CrossRef]
21. Raven, J.A.; Evans, M.C.W.; Korb, R.E. The role of trace metals in photosynthetic electron transport in O_2-evolving organisms. *Photosynth. Res.* **1999**, *60*, 111–150. [CrossRef]
22. Leong, Y.K.; Chang, J.-S. Bioremediation of heavy metals using microalgae: Recent advances and mechanisms. *Bioresour. Technol.* **2020**, *303*, 122886. [CrossRef]
23. Santos, F.M.L.F. Crescimento de Microalgas e Remoção de Nutrientes em Ambientes Poluídos com Metais Pesados. Dissertação Faculdade de Engenharia da Universidade do Porto, Porto, 2017. Repositório Aberto da Universidade do Porto. Available online: https://repositorio-aberto.up.pt/bitstream/10216/106496/2/205643.pdf (accessed on 30 March 2022).
24. Rugnini, L.; Costa, G.; Congestri, R.; Bruno, L. Testing of two different strains of green microalgae for Cu and Ni removal from aqueous media. *Sci. Total Environ.* **2017**, *601–602*, 959–967. [CrossRef]
25. Wu, G.; Cheng, J.; Wei, J.; Huang, J.; Sun, Y.; Zhang, L.; Huang, Y.; Yang, Z. Growth and photosynthetic responses of *Ochromonas gloeopara* to cadmium stress and its capacity to remove cadmium. *Environ. Pollut.* **2021**, *27*, 116496. [CrossRef] [PubMed]
26. Pinto, E.; Carvalho, A.P.; Cardozo, K.H.M.; Malcata, F.X.; Maria dos Anjos, F.; Colepicolo, P. Effect of heavy metals and light levels on the biosynthesis of carotenoids and fatty acids in the macroalgae *Gracilaria tenuistipitata* (varliui Zhang & Xia). *Rev. Bras. Farmacogn.* **2011**, *21*, 349–354. [CrossRef]
27. Silva, J.C.; Echeveste, P.; Lombardi, A.T. Higher biomolecules yield in phytoplankton under copper exposure. *Ecotoxicol. Environ. Saf.* **2018**, *161*, 57–63. [CrossRef] [PubMed]
28. Rocha, G.S.; Parrish, C.C.; Espíndola, E.L.G. Effects of copper on photosynthetic and physiological parameters of a freshwater microalga (*Chlorophyceae*). *Algal Res.* **2021**, *54*, 102223. [CrossRef]
29. Andrade, L.M.; Tito, C.A.; Mascarenhas, C.; Lima, F.A.; Dias, M.; Andrade, C.J.; Mendes, M.A.; Nascimento, C.A.O. *Chlorella vulgaris* phycoremediation at low Cu^{+2} contents: Proteomic profiling of microalgal metabolism related to fatty acids and CO_2 fixation. *Chemosphere* **2021**, *284*, 131272. [CrossRef] [PubMed]
30. Pinto, E.; Sigaud-Kutner, T.C.S.; Leitao, M.A.; Okamoto, O.; Morse, D.; Colepicolo, P. Heavy metal-induced oxidative stress in algae. *J. Phycol.* **2003**, *39*, 1008–1018. [CrossRef]
31. Rezayian, M.; Niknam, V.; Ebrahimzadeh, H. Oxidative damage and antioxidative system in algae. *Toxicol. Rep.* **2019**, *6*, 1309–1313. [CrossRef]
32. Ciero, L.; Bellato, C.M. Proteoma: Avanços recentes em técnicas de eletroforese bidimensional e espectrometria de massa. *Biotecnol. Cienc. Desenvolv.* **2002**, *5*, 158–164.
33. Guarnieri, M.T.; Nag, A.; Yang, S.; Pienkos, P.T. Proteomic analysis of *Chlorella vulgaris*: Potential targets for enhanced lipid accumulation. *J. Proteom.* **2013**, *93*, 245–253. [CrossRef]
34. Abreu, F.C.P.; da Costa, P.N.M.; Brondi, A.M.; Pilau, E.J.; Gozzo, F.C.; Eberlin, M.N.; Trevisan, M.G.; Garcia, J.S. Effects of cadmium and copper biosorption on *Chlorella vulgaris*. *Bull. Environ. Contam. Toxicol.* **2014**, *93*, 405–409. [CrossRef]
35. Bai, X.; Song, H.; Lavoie, M.; Zhu, K.; Su, Y.; Ye, H.; Si, C.; Fu, Z.; Qian, H. Proteomic analyses bring new insights into the effect of a dark stress on lipid biosynthesis in *Phaeodactylum tricornutum*. *Sci. Rep.* **2016**, *6*, 25494. [CrossRef] [PubMed]
36. Gasch, A.P.; Spellman, P.T.; Kao, C.M.; Carmel-Harel, O.; Eisen, M.B.; Storz, G.; Botstein, D.; Brown, P.O. Genomic expression programs in the response of yeast cells to environmental changes. *Mol. Biol. Cell* **2000**, *11*, 4241–4257. [CrossRef] [PubMed]
37. Andersen, R.A. *Algal Culturing Techniques*; Academic Press: San Diego, CA, USA, 2008.
38. Kerby, N.W.; Stewart, W.D.P. The biotechnology of microalgae and cyanobacteria. In *Biochemistry of the Algae and Cyanobacteria*; Rogers, L.J., Gallon, J.R., Eds.; Oxford Clarendon Press: Oxford, UK, 1989; pp. 319–334.
39. Lavens, P.; Sorgeloos, P. *Manual on the Production and Use of Live Food for Aquaculture*; FAO Fisheries Technical Paper No. 361; Food and Agriculture Organization of the United Nations: Rome, Italy, 1996.
40. Henriques, M.; Silva, A.; Rocha, J. Extraction and quantification of pigments from a marine microalga: A simple and reproducible method. *Comm. Curr. Res. Educat. Topics Trends Appl. Microbiol.* **2007**, *2*, 586–593.
41. Veglio, F.; Esposito, A.; Reverberi, A.P. Standardization of heavy metal biosorption tests: Equilibrium and modelling study. *Process Biochem.* **2003**, *38*, 953–961. [CrossRef]

42. Zhang, J.; Xin, L.; Shan, B.; Chen, W.; Xie, M.; Yuen, D.; Zhang, W.; Zhang, Z.; Lajoie, G.A.; Ma, B. PEAKS DB: De Novo sequencing assisted database to search for sensitive and accurate peptide identification. *Mol. Cell. Proteom.* **2012**, *11*, 1–8. [CrossRef]
43. Pradeep, V.; Ginkel, S.W.V.; Park, S.; Igou, T.; Yi, C.; Fu, H.; Johnston, R.; Snell, T.; Chen, Y. Use of copper to selectively inhibit *Brachionus calyciflorus* (predator) growth in *Chlorella kessleri* (prey) mass cultures for algae biodiesel production. *Int. J. Mol. Sci.* **2015**, *16*, 20674–20684. [CrossRef]
44. Heberle, H.; Meirelles, G.V.; Silva, F.R.; Telles, G.P.; Minghim, R. InteractiVenn: A web-based tool for the analysis of sets through Venn diagrams. *BMC Bioinform.* **2015**, *16*, 169. [CrossRef]
45. Andrade, L.M.; Kowalski, P.; Mendes, M.A.; Nascimento, C.A.O. Comparative study of different matrix/solvent systems for the analysis of crude lyophilized microalgal preparations using matrix-assisted laser desorption/ionization time-of-flight mass spectrometry. *Rapid Commun. Mass Spectrom.* **2015**, *29*, 295–303. [CrossRef]
46. Sabatini, S.E.; Juárez, Á.B.; Eppis, M.R.; Bianchi, L.; Luquet, C.L.; Molina, M.C.R. Oxidative stress and antioxidant defenses in two green microalgae exposed to copper. *Ecotoxicol. Environ. Saf.* **2009**, *72*, 1200–1206. [CrossRef]
47. Guanzon, N.G.; Nakahara, H.; Yoshida, Y. Inhibitory effects of heavy metals on growth and photosynthesis of three freshwater microalgae. *Fish. Sci.* **1994**, *60*, 379–384. [CrossRef]
48. Coe, J.C.; Kupitz, C.; Basu, S.; Conrad, C.E.; Roy-Chowdhury, S.; Fromme, R.; Fromme, P. Chapter twenty-two—crystallization of photosystem II for time-resolved structural studies using an X-ray free electron laser. In *Methods in Enzymology: Membrane Proteins-Engineering, Purification and Crystallization*; Shukla, A.K., Ed.; Academic Press: Amsterdam, Holland, 2015; pp. 459–482.
49. Kawakami, K.; Shen, J.-R. Chapter One—Purification of fully active and crystallizable photosystem II from thermophilic cyanobacteria. In *Methods in Enzymology—Enzymes of Energy Technology*; Armstrong, F., Ed.; Academic Press: Amsterdam, Holland, 2018; pp. 1–16.
50. UniProt Consortium. UniProt: A worldwide hub of protein knowledge. *Nucleic Acids Res.* **2019**, *47*, D506–D515. [CrossRef] [PubMed]
51. Irrgang, A.; Weise, C.; Murugaiyan, J.; Roesler, U. Identification of immunodominant proteins of the microalgae *Prototheca* by proteomic analysis. *New Microbes New Infect.* **2015**, *3*, 37–40. [CrossRef] [PubMed]
52. Carrozza, M.J.; Utley, R.T.; Workman, J.L.; Côté, J. The diverse functions of histone acetyltransferase complexes. *Trends Genet.* **2003**, *19*, 321–329. [CrossRef]
53. Barros, D.; Pradhan, A.; Mendes, V.M.; Manadas, B.; Santos, P.M.; Pascoal, C.; Cássio, F. Proteomics and antioxidant enzymes reveal different mechanisms of toxicity induced by ionic and nanoparticulate silver in bacteria. *Environ. Sci. Nano* **2019**, *6*, 1207–1218. [CrossRef]
54. Vingiani, G.M.; Luca, P.; Ianora, A.; Dobson, A.D.W.; Lauritano, C. Microalgal enzymes with biotechnological applications. *Mar. Drugs* **2019**, *17*, 459. [CrossRef]
55. Sauser, K.R.; Liu, J.K.; Wong, T.-Y. Identification of a copper-sensitive ascorbate peroxidase in the unicellular green alga *Selenastrum capricornutum*. *BioMetals* **1997**, *10*, 163–168. [CrossRef]